Water Research 258 (2024) 121655

Contents lists available at ScienceDirect

Water Research

journal homepage: www.elsevier.com/locate/watres

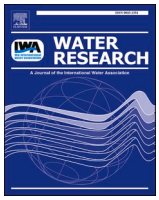

Gas permeable membrane electrode assembly with *in situ* utilization of authigenic acid and base for transmembrane electro-chemisorption to enhance ammonia recovery from wastewater

Zuobin Wang [a,b,c,d], Jiao Zhang [e], Zhiqiang Zhang [a,c,d,*], Qingbo Zhang [b], Beiqi Deng [a,c,d], Nan Zhang [a,c,d], Zhiyong Cao [a,c,d], Guangfeng Wei [f], Siqing Xia [a,c,d]

[a] State Key Laboratory of Pollution Control and Resource Reuse, Key Laboratory of Urban Water Supply, Water Saving and Water Environment Governance in the Yangtze River Delta of Ministry of Water Resources, College of Environmental Science and Engineering, Tongji University, Shanghai 200092, China
[b] National Engineering Research Center of Dredging Technology and Equipment, Key Laboratory of Dredging Technology, CCCC, Shanghai 200082, China
[c] Key Laboratory of Yangtze River Water Environment, Ministry of Education, Tongji University, Shanghai 200092, China
[d] Shanghai Institute of Pollution Control and Ecological Security, Shanghai 200092, China
[e] School of Municipal and Ecological Engineering, Shanghai Urban Construction Vocational College, Shanghai 200432, China
[f] Shanghai Key Laboratory of Chemical Assessment and Sustainability, School of Chemical Science and Engineering, Tongji University, Shanghai 200092, China

ARTICLE INFO

Keywords:
Gas permeable membrane electrode assembly
Authigenic acid and base
In situ utilization
Transmembraneelectro-chemisorption
Ammonia recovery

ABSTRACT

Ammonia recovery from wastewater is of great significance for aquatic ecology safety, human health and carbon emissions reduction. Electrochemical methods have gained increasing attention since the authigenic base and acid of electrochemical systems can be used as stripper and absorbent for transmembrane chemisorption of ammonia, respectively. However, the separation of electrodes and gas permeable membrane (GPM) significantly restricts the ammonia transfer-transformation process and the authigenic acid-base utilization. To break the restrictions, this study developed a gas permeable membrane electrode assembly (GPMEA), which innovatively integrated anode and cathode on each side of GPM through easy phase inversion of polyvinylidene fluoride binder, respectively. With the GPMEA assembled in a stacked transmembrane electro-chemisorption (sTMECS) system, *in situ* utilization of authigenic acid and base for transmembrane electro-chemisorption of ammonia was achieved to enhance the ammonia recovery from wastewater. At current density of 60 A/m^2, the transmembrane ammonia flux of the GPMEA was 693.0 ± 15.0 g N/(m^2·d), which was 86 % and 28 % higher than those of separate GPM and membrane cathode, respectively. The specific energy consumption of the GPMEA was 9.7~16.1 kWh/kg N, which were about 50 % and 25 % lower than that of separate GPM and membrane cathode, respectively. Moreover, the application of GPMEA in the ammonia recovery from wastewater is easy to scale up in the sTMECS system. Accordingly, with the features of excellent performance, energy saving and easy scale-up, the GPMEA showed good prospects in electrochemical ammonia recovery from wastewater.

Abbreviations

ACE	Average current efficiency
AEM	Anion exchange membrane
AnC	Anode chamber
CaC	Cathode chamber
CEM	Cation exchange membrane
DeC	Desalination chamber
DSM	Dimensionally stable mesh
FA	Free ammonia
IEM	Ion exchange membrane
GHG	Greenhouse gas
GPM	Gas permeable membrane
GPMC	Gas permeable membrane cathode
GPMEA	Gas permeable membrane electrode assembly
PTFE	Polytetrafluoroethylene
PVDF	Polyvinylidene fluoride
SEC	Specific energy consumption
SSM	Stainless-steel mesh
sTMECS	Stacked transmembrane electro-chemisorption

* Corresponding author.
E-mail address: zhiqiang@tongji.edu.cn (Z. Zhang).

https://doi.org/10.1016/j.watres.2024.121655
Received 5 March 2024; Received in revised form 18 April 2024; Accepted 20 April 2024
Available online 26 April 2024

TAN Total ammonia nitrogen
TMCS Transmembrane chemisorption
TMECS Transmembrane electro-chemisorption

1. Introduction

Ammonia recovery from wastewater is of great significance for aquatic ecology safety, human health and carbon emissions reduction. Ammonia is one of the most produced chemicals in the world due to its wide applications in various fields, like fertilizers production, chemicals synthesis, pharmaceuticals production, and carbon-free energy storage (Erisman et al., 2008). Ammonia is most synthesized via the Haber-Bosch process transforming atmospheric nitrogen (N_2) into NH_3 (Bodirsky et al., 2014; Deng et al., 2021). Significantly, approximately 2 % of the world's energy consumption and 1.2 % of CO_2 emissions come from the energy-intensive and carbon-intensive ammonia synthesis (Liu et al., 2020; Smith et al., 2020). However, about 40 % of the synthesized ammonia is lost to wastewater as a result of human activity. The ammonia release into the environment can result in eutrophication, which destroys the aquatic ecological environment and threaten human beings' health (Yu et al., 2019). Nitrification-denitrification is the most common process to remove ammonia from wastewater. However, this process just use microorganisms to turn ammonia into N_2 with high energy input (~13 kWh/kg N) (Cruz et al., 2019). Additionally, the emission of N_2O during the process can be responsible for the majority of the carbon footprint of wastewater treatment plants, whereas N_2O is a powerful greenhouse gas (GHG) with a global warming potential 300 times that of CO_2 (Duan et al., 2021; Massara et al., 2017). Accordingly, recovering ammonia from wastewater, especially from strong ammonia wastewater, is a sustainable way of nitrogen utilization (Wang et al., 2019).

The present methods for ammonia recovery from wastewater majorly include air stripping, zeolite adsorption, ion exchange, struvite precipitation, and membrane process (Darestani et al., 2017; Guida et al., 2022; Wu and Vaneeckhaute, 2022). However, they show the defects of high energy consumption, huge chemical input, low efficiency or secondary pollution. For example, air stripping requires a significant base addition and temperature elevation to transform NH_4^+ into free ammonia (FA), as well as a significant acid addition to capture the FA (Liu et al., 2015). Struvite precipitation requires a strict balance of nitrogen, phosphorus, and magnesium. Meanwhile, the consumption of magnesium source accounts for large proportion of struvite cost (Astals et al., 2021; Wang et al., 2020; Z. Wang et al., 2019; Zhang et al., 2019). Due to the benefit of low energy demand, ammonia recovery by gas permeable membrane (GPM) separation has gained great attention in recent years, where ammonia can be captured via the process known as transmembrane chemisorption (TMCS) (Davey et al., 2020; Hou et al., 2019). The membrane process uses less energy to separate NH_3 from liquid. However, it requires large amount of base to raise the influent pH, and require large amount of acid to serve as absorbent for capturing FA (Gonzalez-Salgado et al., 2022).

Due to the fact that OH^- can be continually generated by cathodic reaction and drive the transformation of NH_4^+ into FA in an electrochemical system, the TMCS and electrochemical system have been coupled for ammonia recovery from wastewater (Deng et al., 2023; Kuntke et al., 2017, 2016; Tarpeh et al., 2018). On this basis, we have established the viability of employing electrochemical ammonia membrane absorption systems with GPM and ion exchange membranes (IEM), where the base was generated by cathodic reaction and the acid via water splitting by anode or bipolar membrane (Zhang et al., 2021; Wang et al., 2023, 2024; Cao et al., 2024). However, the ammonia recovery rate in the electrochemical system with separate cathode and GPM can be constrained by the diffusion of FA from the cathode surface to the bulk catholyte (Hou et al., 2018).

Recent studies showed that the use of gas permeable membrane cathode (GPMC) could reduce the above diffusion. A nickel (Ni)-based GPMC manufactured via electroplating Ni on the GPM was reported to boost the ammonia recovery rate by reducing the loss of FA to the bulk catholyte (Hou et al., 2018; Iddya et al., 2020). However, the deposition of nickel may plug the pore of GPM and lower gas permeability, which can result in poor ammonia recovery performance (Iddya et al., 2020). A modified GPMC was developed by binding Ni-functionalized activated carbon on a piece of stainless steel mesh by polyvinylidene fluoride (PVDF) binder (Kim et al., 2021). The porous structure formed during PVDF phase inversion provides enough gas channel for ammonia recovery. However, the Ni catalyst may dissolve in the acidic recovery solution due to the protonation of carbonyl groups on the activated carbon surface, which can result in fast decrease of the electrochemical performance of the electrode (Kim et al., 2018).

On the other hand, the TMCS of ammonia is also influenced by the H^+ concentration on the GPM surface and the diffusion of the generated NH_4^+ to the bulk acid solution (Renard et al., 2004). There is a boundary layer on the GPM surface in the acid solution, where the transmembrane NH_3 immediately reacts with H^+ (Zhang et al., 2020). As ammonia recovery proceeding, the H^+ concentration in this boundary layer decreases, which is unfavorable to the TMCS of ammonia. Besides, slow diffusion of the generated NH_4^+ to the bulk acid solution can arouse accumulation of NH_4^+ on the GPM surface, which also impair the TMCS of ammonia. To obtain sufficient H^+ concentration and fast NH_4^+ diffusion, the conventional TMCS process for ammonia recovery generally maintains excessive H^+ concentration in the absorbent, and rushes the GPM surface through high-speed acid stream recirculation, which means excess demand for acid and energy (Gonzalez-Salgado et al., 2022). In the electrochemical system, H^+ can be continuously generated on the anode surface, and the anode can repulse NH_4^+ via electrostatic interaction. However, the separation of anode and GPM is not helpful to increase the H^+ concentration on the GPM surface and repulse the generated NH_4^+ from the GPM surface to the bulk anolyte.

From the above, separation of electrodes and GPM limit the authigenic chemicals utilization and the ammonia transfer on both wastewater side and absorbent side. Therefore, it is imperative to combine cathode and anode with GPM to construct a composite interface, which couples the *in situ* generation and utilization of acid and base in an electrochemical system for enhanced ammonia recovery. Therefore, this study aimed to develop a gas permeable membrane electrode assembly (GPMEA) with in situ utilization of authigenic acid and base for transmembrane electro-chemisorption (TMECS) to enhance ammonia recovery from wastewater. The surface and electrochemical characteristics of the GPMEA were investigated. The feasibility of its application in recovering ammonia from wastewater was verified. Its performance for ammonia recovery was investigated from multiple perspectives, including in recovery efficiency, ammonia flux and energy consumption. The mechanisms of its enhancing ammonia recovery were further explored. Finally, the implications of the GPMEA for the field of recovering ammonia from wastewater were discussed.

2. Materials and methods

2.1. Materials and chemicals

A commercial hydrophobic expanded polytetrafluoroethylene (PTFE) membrane (0.22 μm pore size, 30 μm thickness; Jufu New Material Technology Co., Ltd, Guangzhou, China), stainless-steel mesh (SSM, 200 mesh, 0.1 mm thickness and 80 μm pore size) and dimensionally stable mesh (DSM; 200-mesh titanium mesh with iridium/tantalum coated) were used to manufacture GPMEA as GPM, cathode and anode, respectively. PVDF powder (600 kDa Mw, Solef 6010, Solvay), N-octanol ($C_8H_{18}O$, reagent grade, Adamas) and N,N-Dimethylacetamide (DMAc, C_4H_9NO, analytical reagent, Greagent) were used to prepare the binder solution. Ammonium sulfate ($(NH)_2SO_4$,

analytical reagent, Greagent) was used for preparation of ammonia solution. Sodium sulfate (Na_2SO_4, analytical reagent, Greagent) was used to prepare salt solution.

2.2. Preparation of gas permeable electrode assembly

The GPMEA consists of a SSM cathode, a DSM anode and a piece of non-conductive GPM. The GPMEA was the integration of SSM cathode and DSM anode separately bonding on each side of GPM by the PVDF binder with a phase-inversion method (**Fig. S1**). In brief, 10 wt% PVDF and 10 wt% N-octanol were dissolved in DMAc, and the solution was stirred at the room temperature for 48 h to obtain a homogeneous binder solution. The prepared solution was coated uniformly on a SSM assembled on an PTFE membrane by a glass rod to manufacture the GPMC. Then the GPMC was immersed in deionized water to induce the phase inversion in coagulation bath for 30 min at room temperature of about 25 ℃. After the coagulation bath, it was immersed in deionized water for 48 h to remove the residual solvent. Then it dried at room temperature of about 25 ℃ for 48 h. To prepare a GPMEA with the GPMC, PVDF binder solution was coated on a DSM assembled on the other side of the GPMC and repeated the above phase-inversion steps.

2.3. Reactor setup and operation

Experiments were conducted in a stacked transmembrane electrochemisorption (sTMECS) system with two units, which was built by stacking two electrochemical desalination cells (EDC) with the names unit 1 (U-1) and unit 2 (U-2), respectively (**Fig. S2**). In the system, each cell consisted of anode chamber (AnC), desalination chamber (DeC), and cathode chamber (CaC). Each chamber had measurements of 4 cm × 4 cm and a 1 cm thickness. In each unit, the AnC and DeC were separated by a piece of anion exchange membrane (AEM, AMI-7001, Membrane International, USA); the DeC and CaC were separated by a piece of cation exchange membrane (CEM, CMI-7000, Membrane International, USA). The CaC of U-1 and the AnC of U-2 were both designated as wastewater chamber and recovery chamber, respectively. The CaC and AnC were separated by either PTEF membrane, GPMC or GPMEA, which was depended on the experiment demand. The above GPM, GPMC or GPMEA was sandwiched between chambers by two piece of 2-mm thick silicone gasket. Each chamber was added in about 20 mL electrolyte. In the AnC of U-1 and CaC of U-2, 150 mM Na_2SO_4 solution was used as electrolyte. Solution of 500 mM Na_2SO_4 was filled in the two DeCs and recirculated at a flow rate of 5 mL/min. Synthetic ammonia-rich wastewater containing 400 mM $(NH_4)_2SO_4$ (about 5500 mg N/L) was added in the CaC, while 6 mM $(NH_4)_2SO_4$ solution was in the AnC.

The impact of electrode style on each side of GPM on ammonia recovery performance were tested in the sTMECS system. The experiment configurations were shown as **Fig. S3**. In group 1 (Control), the cathode of U-1 and the anode of U-2 were SSM cathode and DSM anode respectively, which were placed separately from the GPM. In group 2, the GPMC that consist of cathode and GPM was employed as the cathode of U-1, and the anode of U-2 was DSM anode placed separately from the GPMC. In group 3, the GPMEA with cathode-GPM-anode sandwich structure was employed as the cathode of U-1 and the anode of U-2. Constant current densities (15, 30, 60, and 120 A/m^2) were applied to each unit by two independent power supplies. During the 2-h operation, unit voltages were monitored, and the $NH_4^+ - N$ concentration and pH were measured intermittently. The whole experiments were operated at the temperature of 25 ℃.

2.4. Analyses and calculations

The hydrophobicity of the GPMC or the GPMEA surfaces was determined by contact angle measurements (JY-82, Dingsheng, China). Their surface morphologies were visualized using a scanning electron microscope (SEM, GeminSEM 300, Zeiss, Germany). Three kinds of electrochemical analyses including electrochemical impedance spectroscopy (EIS), linear sweep voltammetry (LSV), and cyclic voltammetry (CV) were conducted to characterize raw electrode, GPMC and GPMEA in a 500 mM Na_2SO_4 solution by using a potentiostat (VoltLab 40 PGZ301, Hach, USA). EIS was conducted under open circuit conditions by applying an impedance amplitude of 10 mV with a frequency ranged from100 kHz to 0.01 Hz. A potential ranged from −3.0 to 0.3 V was applied to SSM cathode or the cathodic side of GPMC or GPMEA while a potential ranged from −0.3 V to 3.0 V was applied to DSM anode or anodic side of GPMEA in the analyze of LSV with a scan rate of 10 mV/s. CV was conducted using the same scan rate with a potential ranged from −0.8 V to 0.8 V. AgCl electrode acted as a reference electrode while a piece of Pt mesh electrode was employed as a counter electrode during these electrochemical analyses.

Liquid samples were collected from CaC of U-1 and AnC of U-2 every 30 min during the 2-h operation. The concentrations of $NH_4^+ - N$ in the samples were determined by using a spectrophotometry (UV-2700, Shimadzu, Japan). The pHs in the CaC and AnC were monitored by using a pH probe (LabSen241–3, Sanxin, China). All tests were repeated three times and the average value of test results was taken.

Recovery efficiency (E_{rc} (t), %) and removal efficiency (E_{rm} (t), %) of ammonia from wastewater were calculated by Eqs. (1) and (2), respectively.

$$\mathrm{E_{rc}}(t) = \frac{(c_{\mathrm{AnC}}(t) - c_{\mathrm{AnC}}(0))V_{\mathrm{AnC}}}{c_{\mathrm{CaC}}(0)V_{\mathrm{CaC}}} \times 100\% \quad (1)$$

$$\mathrm{E_{rm}}(t) = \frac{c_{\mathrm{CaC}}(0) - c_{\mathrm{CaC}}(t)}{c_{\mathrm{CaC}}(0)} \times 100\% \quad (2)$$

where $c_{\mathrm{AnC}}(0)$ and $c_{\mathrm{AnC}}(t)$ are the $NH_4^+ - N$ concentrations (mg N/L) in the AnC at initial time and operation time t (h), respectively; $c_{\mathrm{CaC}}(0)$ and $c_{\mathrm{CaC}}(t)$ are the $NH_4^+ - N$ concentrations (mg N/L) in the CaC at initial time and operation time t (h), respectively; V_{AnC} and V_{CaC} are the volumes (L) of anolyte and catholyte, respectively.

In the bulk catholyte, the ratio of FA over total ammonia nitrogen is determined by the bulk catholyte pH when the temperature is constant. Thus, the fraction of NH_3 ($\alpha(t)$) can be calculated by Eq. (3):

$$\alpha(t) = \frac{K_a}{K_a + 10^{-\mathrm{pH_{catholyte}}(t)}} \quad (3)$$

where K_a is the dissociation constant of NH_4^+ and $\mathrm{pH_{catholyte}}$ (t) is the bulk catholyte pH.

To further evaluate the ammonia recovery performance of the system with different electrode style on each side of GPM, the transmembrane ammonia flux in the operation duration (J_N (t), g N/(m^2·d)) was calculated by diving the mass of recovered ammonia in the AnC over the working area of the GPMEA (A_{GPMEA}, m^2) (Eq. (4)):

$$J_N(t) = \frac{24 \cdot (c_{\mathrm{AnC}}(t) - c_{\mathrm{AnC}}(0))V_{\mathrm{AnC}}}{1000 \cdot A_{\mathrm{GPMEA}} t} \quad (4)$$

The specific energy consumption (SEC, kWh/kg N) of the sTMECS system was defined as Eq. (5) including the energy consumption of pumps for electrolyte circulation (Zhang et al., 2013).

$$\mathrm{SEC} = \frac{1000 \cdot \sum_j i A_{\mathrm{GPMEA}} \int_0^t U_j(t)\mathrm{d}t + nQ\gamma Et \Big/ 1000}{(c_{\mathrm{AnC}}(t) - c_{\mathrm{AnC}}(0))V_{\mathrm{AnC}}} \quad (5)$$

where i is the current density (A/m^2), U_j (t) is the monitored voltage (V) of each unit at operation time t (h), and subscript j represents the two units; n is the number of peristaltic pump, Q is flow rate (m^3/s), γ is 9800 N/m^3, and E is the hydraulic pressure head (m).

The partial pressure of ammonia determines rates of the mass transfer of ammonia as well as the absorption reaction. For the ammonia

absorption reaction in the TMECS process, subsequent reaction rate is controlled by the rate of diffusion of the reaction product NH_4^+ to the bulk anolyte (Renard et al., 2004). The NH_3 partial pressure can be presented by given by Eq. (6).

$$p_{NH_3} = \frac{100\lambda m_{NH_3}}{K_H} \quad (6)$$

where λ is the activity coefficient of ammonia and can be assumed to be equal to 1 for ammonia concentrations below 50 g/L; $m_{NH3}$is the molar concentration of ammonia and K_H is the Henry's law constant.

Moreover, the analyses of the local pH of electrode, the mass transfer coefficients of ammonia (**Table S1**, calculated based on the results from **Fig. S4**) and the average current efficiency (ACE) of the sTMECS system were presented in the **Section S2** of the **Supplementary Information**.

3. Results and discussion

3.1. Characteristics of the GPMEA

Contact angle analyses and SEM morphological images of the GPMEA are shown in Fig. 1 and Fig. S5, respectively. The unprocessed PTFE membrane displayed a superhydrophobic surface with a contact angle of 119 ± 5° (Fig. 1a). After attaching SSM cathode on the PTFE membrane with PVDF binder, the contact angle of the surface facing the CaC reduced to 92 ± 1°. The contact angle of the surface facing the AnC decreased to 84 ± 1° after bonding DSM anode on the membrane (Fig. 1b-c). Thus, the integration of PTFE membrane, SSM cathode and DSM anode by phase-innversion PVDF binder had an obvious effect on the hydrophobicity of each side surfaces of the GPM. The decrease of contact angles could be attributed to the exposure of SSM cathode and DSM anode. According to the SEM microscopic graphs of the two surfaces, the hydrophilic surfaces of the metal mesh were partially exposed out of PVDF binder (Fig. 1e-f). The GPMEA surfaces were typical porous

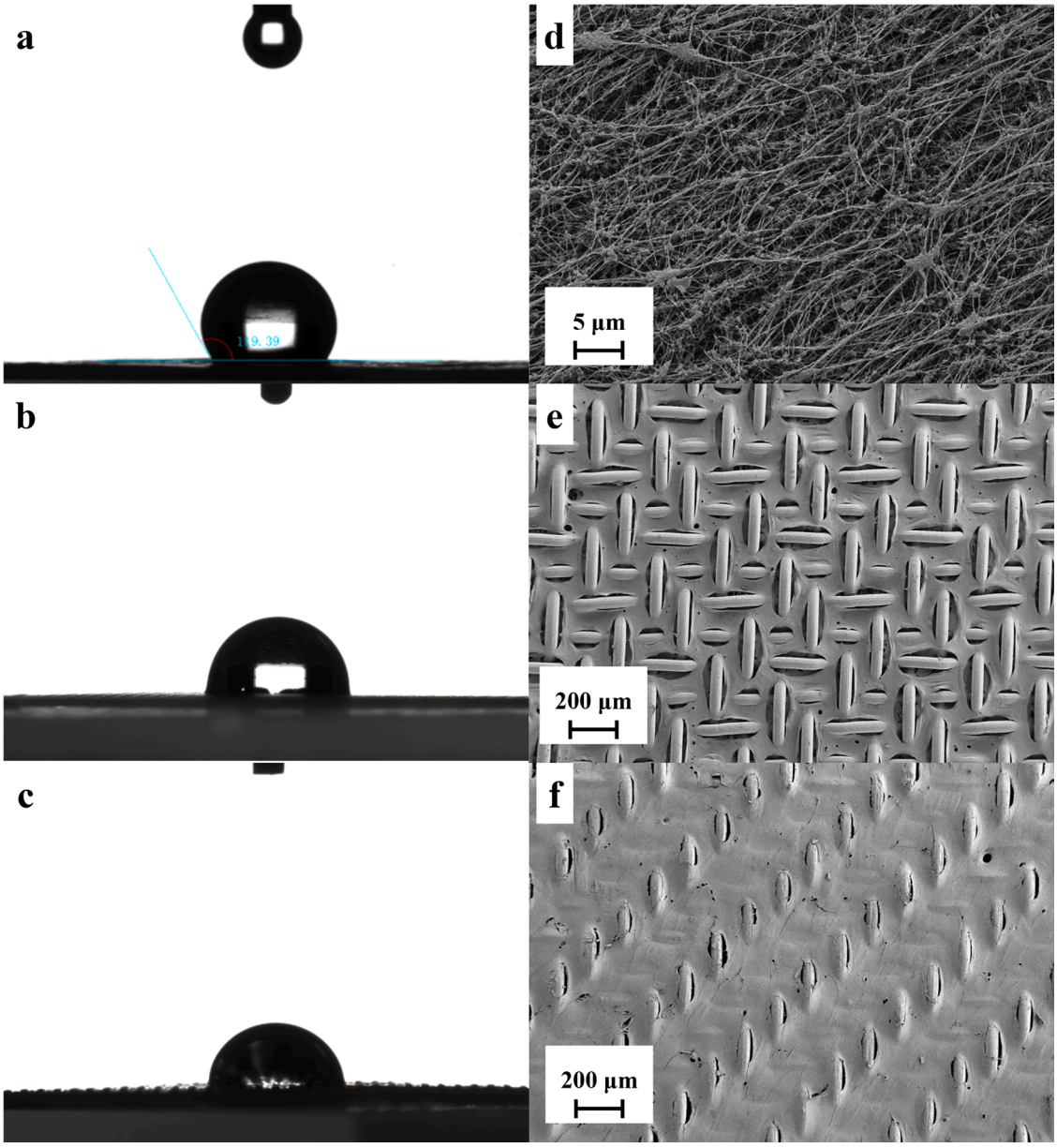

Fig. 1. Contact angle measurements and SEM images of (a) (b) surface of raw PTFE membrane, (c) (d) surface of GPMEA facing to CaC, and (e) (f) surface of GPMEA facing to AnC.

structure, which could provide more channels for transmembrane mass transfer of ammonia (**Fig. S5a-b**). On the basis of cross-section SEM images, the thickness of GPMEA was determined to be 240 ± 5 μm, which was thicker than the PTFE membrane (30 μm) and the GPMC (135 ± 5 μm) (**Fig. S5c-d**).

The EIS analyses demonstrated that the ohmic resistance (R_Ω) of SSM cathode was slightly increased from 6.4 Ω to 10.4 Ω after bonding cathode on GPM by PVDF binder, while charge transfer resistance (R_{ct}) slightly decreased from 52.7 Ω to 50.6 Ω (Fig. 2a). Both R_Ω and R_{ct} of DSM anode after bonding with GPM were increased. The R_Ω of the DSM anode increased from 5.1 Ω to 7.6 Ω while the R_{ct} increased from 0.4 Ω to 6.1 Ω (Fig. 2b). LSV measurements reveal that there was no appreciable difference between the SSM cathode and the GPMC in terms of the polarization curves and hydrogen evolution potential (−1.04 V), which was consistent with the result of EIS (Fig. 2**c-d**). The electrochemical performance of the SSM cathode did not appear to be significantly impacted by the PVDF binder (Li et al., 2021). However, following DSM anode bonded to the GPM by PVDF binder, the oxygen evolution potential increased somewhat, rising from 1.77 V to 1.80 V. There was no significant difference in the CV curves of SSM and DSM anode before and after bonding to the GPM (**Fig. S6**).

3.2. Feasibility of the GPMEA recovering ammonia

We tested the ammonia recovery feasibility via the GPMEA in the sTMECS system at a 60 A/m^2 electric current density. As shown in Fig. 3a, we obtained 88.4 ± 4.7 % recovery and 89.5 ± 5.3 % removal of ammonia. The recovery and the removal efficiency were generally consistent, indicating that little $NH_4^+ - N$ entered the DeC via back diffusion driven by the NH_4^+ concentration gradient between the CaC and DeC. The bulk catholyte pH was below 9.3 within 45 min, which was lower than the pK_a of NH_4^+ (Fig. 3b). However, the ammonia recovery process has started at least 0.5 h according to Fig. 3a, indicating that the local pH in the vicinity of the GPMEA cathode might drive the ammonium-ammonia transformation and enabled the TMECS of ammonia to occur. As the system operated, the pH in the CaC continued to rise above 10.0 while the pH in the AnC decreased to below 2.0. According to the above, the feasibility of ammonia recovery by the GPMEA with authigenic acid and base can be confirmed.

The ammonia recovery performance of the GPMEA at various current densities was investigated in the sTMECS system. At increasing current densities, higher ammonia recovery efficiency and more recovered ammonia mass in the AnC were obtained (Fig. 4**a-b**), which was similar with the reported studies (Li et al., 2021; Rodríguez Arredondo et al.,

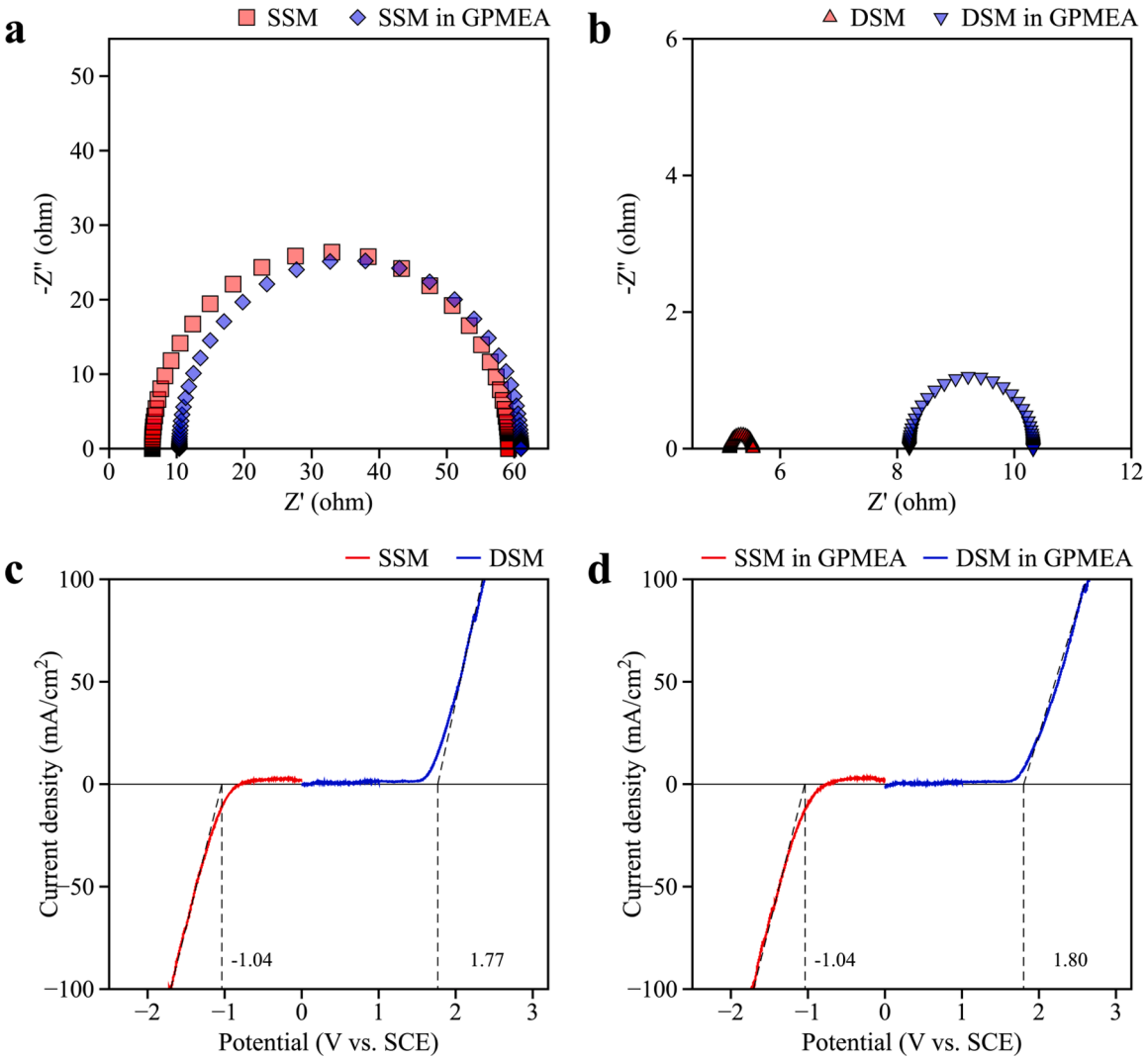

Fig. 2. EIS analyses of (a) SSM cathode and (b) DSM anode before and after bonding with the GPM by PVDF binder (open circuit, 10 mV impedance amplitude, and 100 kHz to 0.01 Hz frequency range); LSV curves of SSM cathode and DSM anode (c) before and (d) after bonding with the GPM (potential range of −3.0 to 0.3 V on SSM and 0.3 V to 3.0 V on DSM, 10 mV/s scan rate).

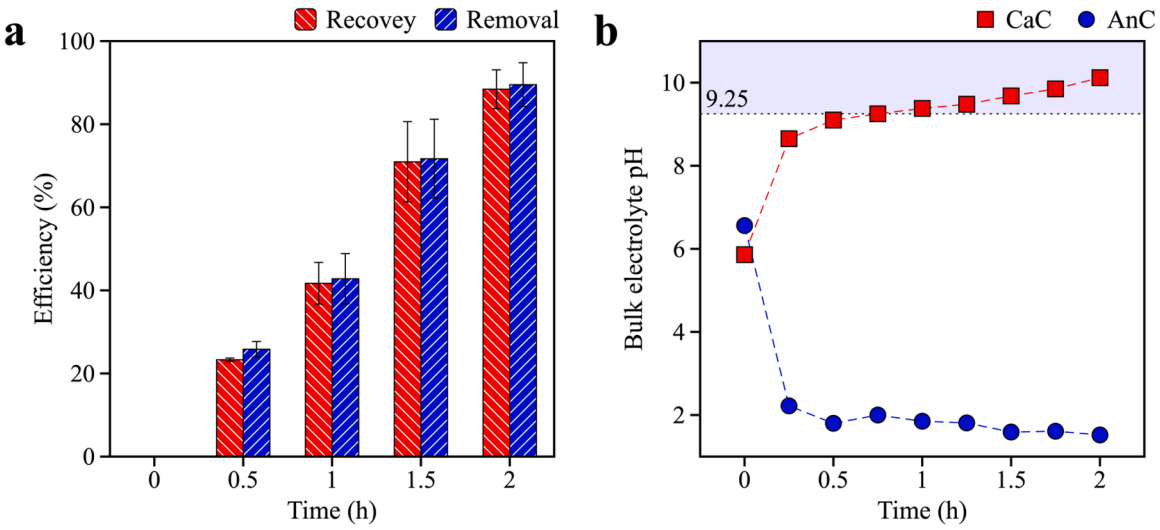

Fig. 3. Ammonia recovery performance of the GPMEA at 60 A/m^2 current density: (a) ammonia recovery and removal efficiency; (b) bulk electrolyte pH.

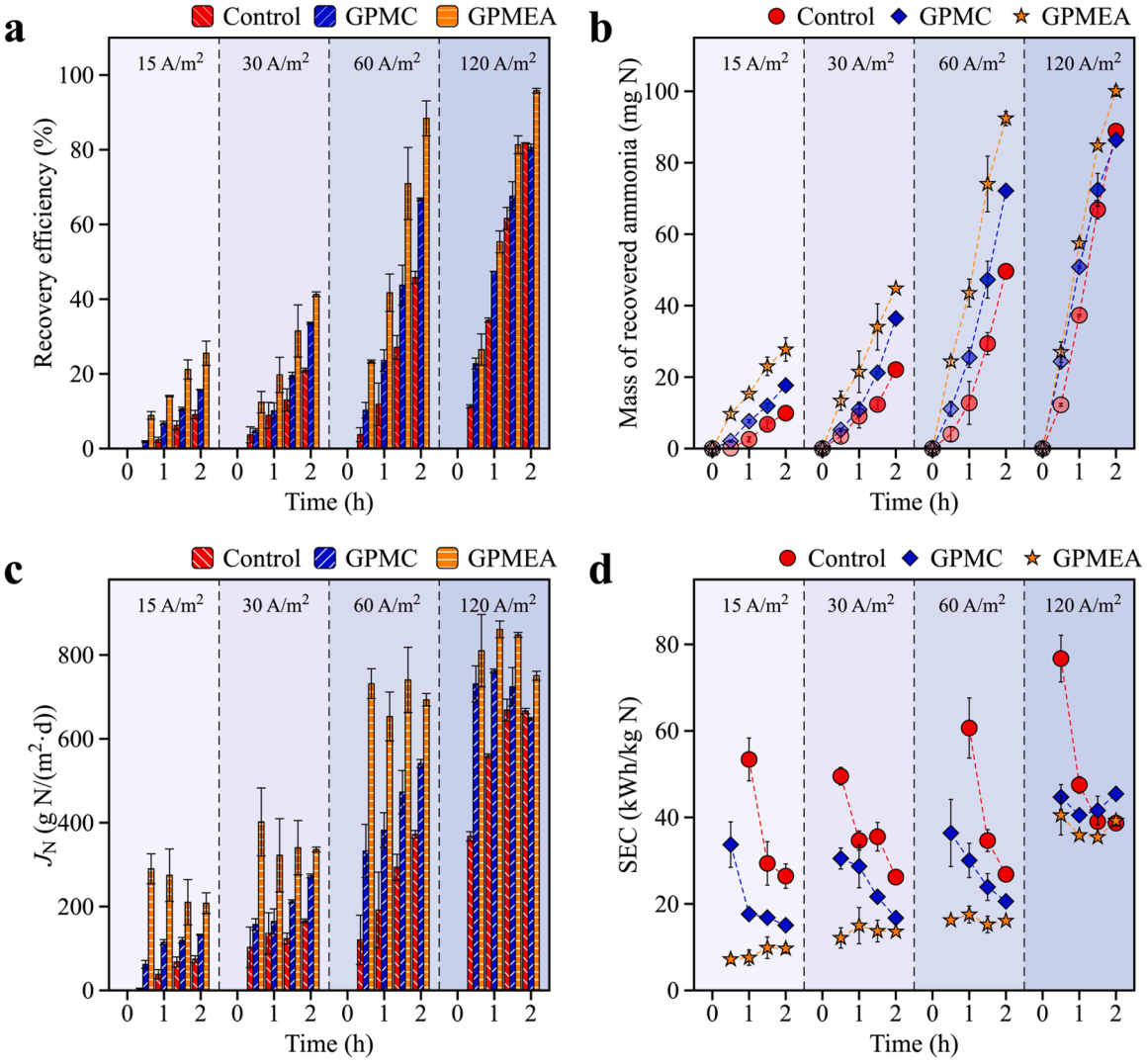

Fig. 4. (a) Ammonia recovery efficiency; (b) mass of recovered ammonia in the AnC; (c) transmembrane ammonia flux; and (d) specific energy consumption for ammonia recovery with different types of electrodes at various constant current densities.

2017). The speedy electrode reactions at high current densities promoted the generation of OH^- and H^+, whose *in situ* utilization promoted the transfer-transformation process of ammonia, which was responsible for the enhanced ammonia recovery. The bulk catholyte pH at 15 A/m^2 was only 8.8, which was lower than the pK_a (9.3) of NH_4^+ dissociation. The ratio of FA in the bulk catholyte was only 24 % after 2-h operation (**Fig. S7a-c**). At 60 A/m^2, the pH in CaC was promoted to 10.1 after 2-h operation and the ratio of FA was sharply increased to 88 %. However, the end pH in CaC was 12.7 after 2 h operation and the ratio of FA was about 99 % at 120 A/m^2. The E_N was only promoted to 95.8 ± 0.6 % when the current density was increased from 60 A/m^2 to 120 A/m^2. The recovered ammonia mass in the AnC at 120 A/m^2 was only increased from 92.4 ± 2.0 mg N to 100.1 ± 1.4 mg N by 8.2 % compared with that at 60 A/m^2 speedy electrode reactions at high current densities.

3.3. Enhanced TMECS ammonia recovery by the GPMEA

3.3.1. Ammonia recovery efficiency

The results shown in Fig. 4 also demonstrates that ammonia recovery was enhanced by the GPMEA in the sTMECS system. The GPMEA could promote the recovery process at all electric current density conditions. For instance, the recovery efficiency of GPMEA was 88.4 ± 4.7 % at 60 A/m^2 current density, which was significantly higher than that in Control (45.8 ± 1.6 %) and the GPMC (66.7 ± 0.4 %) experiments. The recovered ammonia mass in the AnC with the GPMEA was 92.4 ± 2.0 mg N, higher than 49.6 ± 1.2 mg N in the Control experiment and 72.1 ± 1.3 mg N in the GPMC experiment. Combining the cathode with the GPM could take advantage of the local pH on the cathodic surface to enable *in-situ* generation and utilization of OH^-, which could reduce the difussion of FA and OH^- from the cathode surface to the bulk catholyte and thus enhance ammonia recovery (Hou et al., 2018). However, the performance of the GPMC at high current density was not discussed in the prior study that employed Ni-based GPMCs (Hou et al., 2018; Iddya et al., 2020). According to the results in this study, the strengthening effect of the GPMC on ammonia recovery was significantly weakened at high electric current density of 120 A/m^2 while the GPMEA still presented a significant enhancement effect on the ammonia recovery. At the current density of 120 A/m^2, the GPMEA had an enhancing effect throughout the entire operation, whereas the GPMC appeared to only have a strengthening effect on ammonia recovery in the early stages of operation. The eventual ammonia recovery of the GPMEA was 95.8 ± 0.6 %, compared to about 80 % of recovery efficiencies in Control and GPMC experiments. Obviously, by bonding the DSM anode, the GPMEA could break through the bottleneck of individual GPMC on enhancing ammonia recovery at high current density.

3.3.2. Transmembrane ammonia flux

We further calculated J_N in the sTMECS system with the GPMEA applied at various current density (Fig. 4c). At 15 A/m^2 current density, the 2-h J_N in the GPMEA experiment was 207.9 ± 24.6 g N/(m^2·d). The average J_N was dramatically promoted to 692.9 ± 15.0 g N/(m^2·d) after the current density increased to 60 A/m^2. A slight promotion of J_N to 750.5 ± 10.7 g N/(m^2·d) was obtained at the current density of 120 A/m^2.

According to the results of controlled trials, the GPMEA could increase J_N by 123 ± 50 % and36 ± 18 % compared with the separate electrodes and GPMC at current density from 15 to 60 A/m^2 (Fig. 4**c** and **Fig. S8a**). At 15 A/m^2 current density, the 2-h J_N in the GPMEA experiment was 208.0 ± 25.0 g N/(m^2·d), which was 180 % and 57 % higher than those in Control (74.3 ± 8.2 g N/(m^2·d)) and GPMC (133.0 ± 1.3 g N/(m^2·d)) experiments, respectively. At 60 A/m^2 current density, J_N of the GPMEA (693.0 ± 15.0 g N/(m^2·d)) was 86 % and 28 % higher those of the Control (372.0 ± 9.3 g N/(m^2·d)) and the GPMC (541.0 ± 9.6 g N/(m^2·d)), respectively. Compared with the reported Ni-based GPMC and Ni/AC GPMC, the GPMEA also showed superiority in the transmembrane ammonia flux. For example, the flux at 15 A/m^2 was about 48 % higher than that of the Ni/AC GPMC (Kim et al., 2021).

The great improvement in transmembrane ammonia flux might be attributed to the advantage of the reactor configuration of the sTMECS system and the *in situ* utilization of anodic H^+. H^+ could be generated continuously via anodic reaction and reacted with FA on the surface of GPM timely, which maintained the partial pressure of NH_3 over the membrane in this study. The previous study usually used acid solution (e.g., H_2SO_4, HNO_3) at a certain concentration as absorbent, where the H^+ was continuously consumed pH increasing (Hou et al., 2018; Iddya et al., 2020). High pH of recovery solution had an adverse effect on ammonia recovery via electrochemical membrane separation (Kim et al., 2021). A high J_N of about 400 g N/(m^2·d) at 100 A/m^2 has been reported, in which ammonia recovery was achieved with online acid and base generation via a bipolar membrane electrodialysis combined with membrane contactor (Li et al., 2021). In this study, the transmembrane ammonia flux was increased with current density at all experiments. The GPMEA still showed good enhancement for transmembrane mass transfer of ammonia at high current densities. The 2-h J_N of the GPMEA could reach 751.0 ± 11.0 g N/(m^2·d) at 120 A/m^2 current density while the flux in Control and GPMC experiments were both ~650 g N/(m^2·d).

3.3.3. Energy consumption

The SEC for ammonia recovery is shown in Fig. 4d. In the GPMEA experiments, the SEC increased with the promoted electric current density. The SEC for ammonia recovery could be low as 9.7 ± 1.1 kWh/kg N at the current density of 15 A/m^2. It increased to 13.6 ± 0.4, 16.1 ± 0.6, and 39.2 ± 1.2 kWh/kg N respectively when the current density was promoted to 30, 60, and 120 A/m^2.

The GPMEA could significantly reduce the SECs for ammonia recovery in the sTMECS system at various current density compared with the separate electrodes or GPMC, especially at the early period of the recovery process (Fig. 4**d**). At the current density of 15, 30, and 60 A/m^2, the SECs in GPMEA experiments were significantly decreased by 50 ± 12 % and 25 ± 9 % compared with that in the Control and GPMC experiments, respectively (**Fig. S8b**). The SEC of GPMEA at 15 A/m^2 was 9.7 ± 1.1 kWh/kg N, which was decreased by ~63 % and ~36 % compared with the separate electrode and GPMC, respectively. Compared with the SEC for ammonia recovery (~23 kWh/kg N at 14.3 A/m^2) of the Ni/AC GPMC in the previous reported study, the GPMEA also has significant advantages of lower energy consumption (Hou et al., 2018; Iddya et al., 2020; Kim et al., 2021). Compared with the Haber-Bosch process and stripping processes (including air stripping and vacuum stripping), ammonia recovery via the sTMECS system with GPMEA shows significant advantage on theSEC and GHG emissions (**Table S2**). Even though the sTMECS system may have similar SEC with conventional TMCS processes in some cases, the GHG emissions generated by pH adjustment can be avoided in the sTMESC system, which makes its carbon emissions much lower.

With the current density further increasing to 120 A/m^2, the average SECs of 2-h operation in the three experiment groups had little difference. In this case, GPMEA only showed obvious advantage on energy consumption at the early stage of the operations, where the 2-h average SECs just had slight difference among GPMEA, GPMC and separate electrodes (Fig. 4**d**). On the basis of the 2-h average SEC and the average J_N at 120 A/m^2 current density (**Fig. S8b**), it was clearly demonstrated that the effects of GPMEA on reducing energy consumption was not significant at high current density. But the GPMEA could still maintain a higher average J_N at high current density than both separate electrodes and GPMC.

In summary, this study demonstrated that electrochemical ammonia recovery using the GPMEA is promising to achieve high N recovery efficiency. Moreover, compared with the conventional electrodes and the GPMC, the GPMEA in this study showed average 123 ± 50 % and 36 ± 18 % increase in J_N, and 50 ± 12 % and 25 ± 9 % decrease in SEC at different current density by minimizing the distance between the

electrodes and GPM (**Fig. S8**).

3.4. Mechanisms of enhanced electrochemical ammonia recovery by the GPMEA

3.4.1. In situ generation and utilization of OH^- and H^+

In the closed-circuit condition, the NH_4^+ can be attracted to the cathode and enriched on the cathode surface due to the negative charge on the cathode surface (Kuchena and Wang, 2020; Kywe and Ratanatamskul, 2022). Furthermore, local high pH on the cathode surface due to the *in situ* generation of OH^- via the cathode half reaction of water splitting: $2H_2O+2e^-\rightarrow H_2\uparrow+2OH^-$. As Fig. 5**a-b** shown, the local pH in the cathode boundary layer (10–100 μm thickness) can be over 10.5, which was much higher than the pH in the bulk catholyte as well as the pK_a of NH_4^+ dissociation. The enriched NH_4^+ on the cathode surface were *in situ* transformed into FA in this high pH environment and the ratio of c_{FN}/c_{TAN} was much higher than that in the bulk catholyte.

In the conventional TMCS process, the FA coming across the GPM can be absorbed and continuously consume the H^+ in the boundary layer, resulting in a lower H^+ concentration than that in the bulk acid solution. Generally, the flow rate of the absorb solution was increased to reduce the thickness of the boundary layer and maintain enough H^+ for the FA absorption (Asfand et al., 2016). In this study, H^+ can be continuously generated by the anode reaction: $2H_2O\rightarrow O_2\uparrow+4H^++4e^-$. The FA can immediately react with the H^+ on the anode surface of the GPMEA: $NH_3 + H^+\rightarrow NH_4^+$. By coupling the GPM to the electrodes, the H^+ can be continuously provided for ammonia absorption. Furthermore, the H^+ concentration nearby the anode surface was higher than that in the bulk anolyte, which could accelerate the reaction rate of ammonia absorption (Fig. 5c). On the other hand, NH_4^+ generated by the absorption reaction can be repulsed to the bulk anolyte by the anode due to the electrostatic interaction, which can reduce the NH_4^+ accumulation in the reaction interface of ammonia absorption and further accelerate the ammonia absorption (Renard et al., 2004).

3.4.2. Enhanced transmembrane mass transfer of ammonia

The coupling between the electrode reaction interface and the TMCS interface increases the transmembrane pressure difference of NH_3 and enhances the transmembrane mass transfer of ammonia. In the sTMECS system, the transmembrane mass transfer of ammonia consists of three steps (Gonzalez-Salgado et al., 2022; Mansourizadeh et al., 2022): (i) FA generated nearby the cathode surface and transferred to the GPM surface; (ii) transmembrane mass transfer of FA; (iii) absorption of FA by the acid solution. Generally, the NH_3 partial pressure can be neglected due to the instantaneous ammonia absorption reaction (Kywe and Ratanatamskul, 2022). As mentioned earlier, GPMEA can elevate the

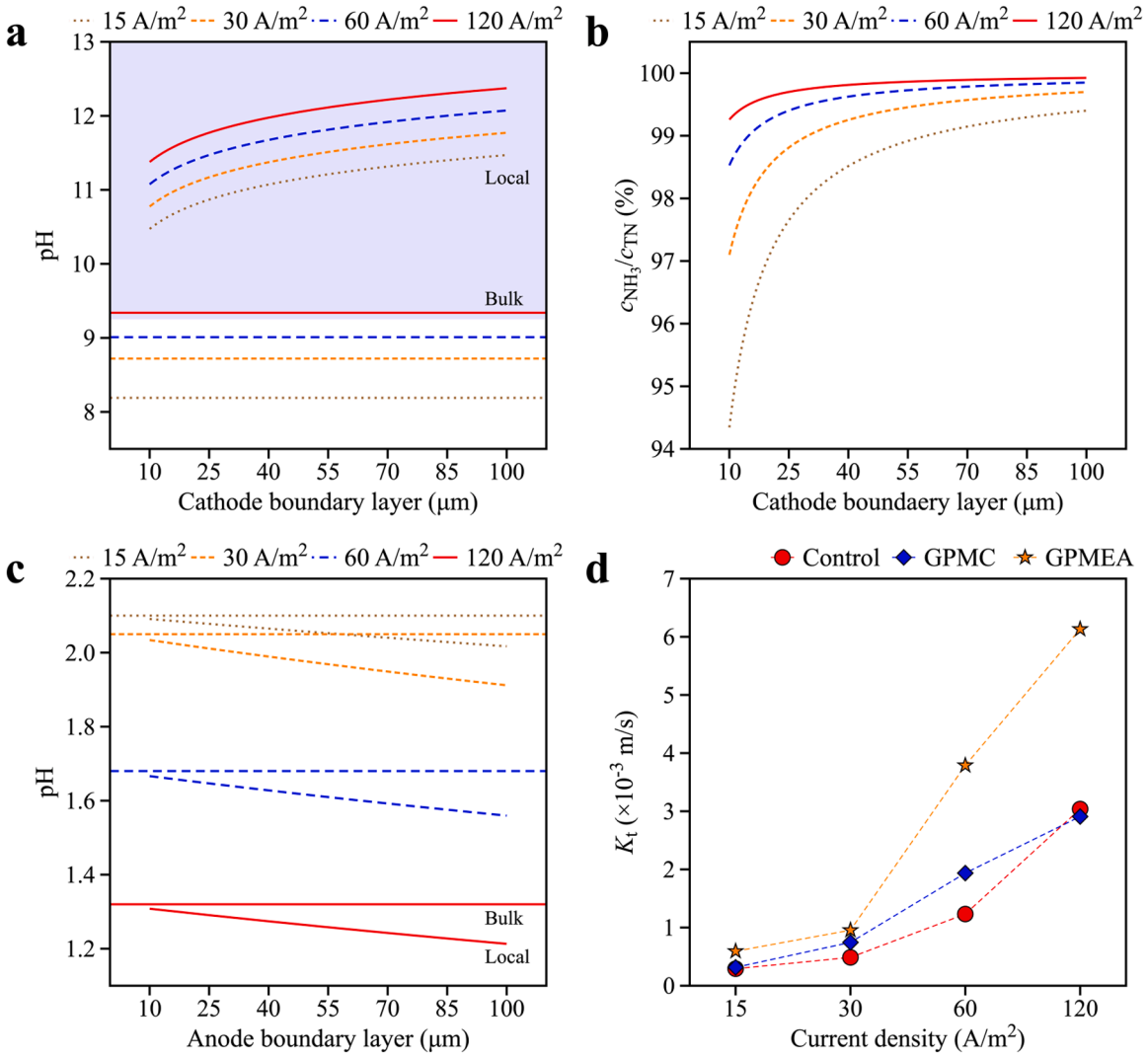

Fig. 5. (a) local pH and (b) ammonia ratio in the cathode boundary layer (0.5 h, colored section indicated pH above pK_a of NH_4^+ dissociation); (c) local pH in the anode boundary layer (0.5 h); and (d) enhanced transmembrane mass transfer of ammonia by the GPMEA.

ammonia concentration on the GPM surface in the CaC and increase the NH_3 partial pressure based on Eq. (6). According to the total mass transfer coefficient of ammonia, the transmembrane mass transfer of ammonia can be enhanced by the GPMEA at various electric current densities (Fig. 5d).

3.4.3. Improved average current efficiency

The ACE can reveal the electron utilization efficiency of the system during the ammonia recovery process (Chen et al., 2021). As shown in **Fig. S9**, the GPMEA can significantly promote the ACE for ammonia recovery in the sTMECS system. At the various current densities from 15~60 A/m^2, the ACEs in GPMEA experiments were above 90 % while in Control experiments were just range from 40 % to 50 %. In terms of the electrode reactions, the molar amounts of OH^- and H^+ generated by the electrode reactions are assumed equal to the electron amount in the electric circuit. Under this premise, the ACE can also reveal the utilization efficiency of OH^- and H^+. By *in situ* generation and utilization of OH^- and H^+, the GPMEA can promote the utilization efficiency of electrons, which is beneficial to enhance the ammonia recovery and reduce the energy consumption.

In short, the mechanisms of enhanced ammonia recovery by the GPMEA can be illustrated as Fig. 6. The cathode of the GPMEA can capture NH_4^+ from the bulk wastewater to its surface via the electrostatic attraction, and provide an localized extreme high pH zone on the cathode side to make ammonium transform into FA via the authigenic base, which is helpful to remove ammonia from wastewater. At the same time, the anode of the GPMEA can provide a localized extreme low pH zone on the anode side to enhance the TMECS of FA via the authigenic acid, and eject NH_4^+ from its surface to the bulk anolyte via the electrostatic repulsion, which is helpful to concentrate the recovered ammonia.

3.5. Implications

The above results indicate that the GPMEA can be used in the sTMECS system for energy-effective ammonia recovery from wastewater in a low carbon emission way. Compared with conventional ammonia recovery processes that need pH adjustment, the use of GPMEA in the sTMECS system can maximize the utilization of authigenic acid and base generated by electrode reactions, reducing GHG emissions from exogenous inputs of acid and base (**Table S2**). Even compared to similar electrochemical technologies for ammonia recovery, the shortened membrane-electrode distance by GPMEA enables the sTMECS system to achieve higher energy utilization efficiency. For practical application, the combination of GPMEA and the sTMECS system can leverage the advantages of stackability to achieve easy scale-up (**Fig. S10**). On the other hand, it is advisable to explore appropriate pre-treatment methods to mitigate the adverse effects of inorganic scaling (primarily induced by Ca^{2+} and Mg^{2+}) on the membranes (both GPMEA and IEMs) resulting from the intricate composition of real wastewater. As for the biofouling, the electrostatic repulsion due to the negative potential on the GPMEA cathode can repelled the negatively charged organics and microbes (Ren et al., 2023). Moreover, the high pH of the catholyte is beneficial to inhibit the growth of microbes. These can effectively reduce biofouling of the GPMEA.

4. Conclusions

This proof-of-concept study has demonstrated that electrochemical ammonia recovery using the GPMEA is promising to achieve high N recovery efficiency. The GPMEA enhanced the transmembrane mass transfer of ammonia and improved current efficiency via *in situ* generation and utilization of OH^- and H^+. Significantly, more work can be done in optimizing the GPMEA and promoting practical applications. To regulate the GPMEA properties such as porosity, thickness and internal structure, the formulation of binder solution and the operating conditions of phase inversion process can be further improved. Besides, the GPMEA assembled in the sTMECS system showed the easy scale-up potential for large-scale application by stacking the TMECS units. Nevertheless, the GPMEA fouling caused by inorganic and organic components in the real ammonia-rich wastewater should be investigated in the further study.

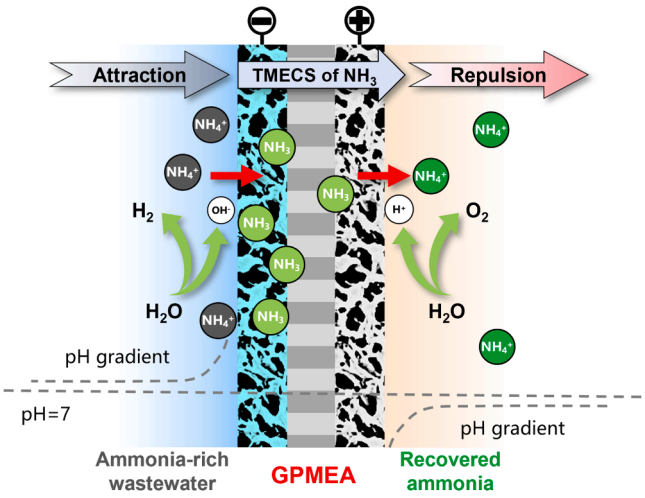

Fig. 6. Mechanism illustration of the GPMEA enhancing ammonia recovery from wastewater.

CRediT authorship contribution statement

Zuobin Wang: Writing – review & editing, Writing – original draft, Methodology. **Jiao Zhang:** Validation, Funding acquisition. **Zhiqiang Zhang:** Writing – review & editing, Supervision, Funding acquisition. **Qingbo Zhang:** Supervision. **Beiqi Deng:** Validation, Investigation. **Nan Zhang:** Validation, Investigation. **Zhiyong Cao:** Validation, Investigation. **Guangfeng Wei:** Supervision, Funding acquisition. **Siqing Xia:** Supervision, Funding acquisition.

Declaration of competing interest

The authors declare that they have no known competing financial interests or personal relationships that could have appeared to influence the work reported in this paper.

Data availability

Data will be made available on request.

Acknowledgments

This work was supported by Natural Science Foundation of Shanghai, China (No. 21ZR1468700, No. 20ZR1418900); the Foundation of State Key Laboratory of Pollution Control and Resource Reuse (Tongji University) (No. 2022-4-YB-07); Key Laboratory of Urban Water Supply, Water Saving and Water Environment Governance in the Yangtze River Delta of Ministry of Water Resources, Tongji University; Key Laboratory of Dredging Technology, CCCC, China; Fundamental Research Funds for the Central Universities, China; and National Key Research and Development Program of China (No. 2021YFC3201301).

Supplementary materials

Supplementary material associated with this article can be found, in

the online version, at doi:10.1016/j.watres.2024.121655.

References

Asfand, F., Stiriba, Y., Bourouis, M., 2016. Impact of the solution channel thickness while investigating the effect of membrane characteristics and operating conditions on the performance of water-LiBr membrane-based absorbers. Appl. Therm. Engin. 108, 866–877.

Astals, S., Martínez-Martorell, M., Huete-Hernández, S., Aguilar-Pozo, V.B., Dosta, J., Chimenos, J.M., 2021. Nitrogen recovery from pig slurry by struvite precipitation using a low-cost magnesium oxide. Sci. Total Environ. 768, 144284.

Bodirsky, B.L., Popp, A., Lotze-Campen, H., Dietrich, J.P., Rolinski, S., Weindl, I., Schmitz, C., Müller, C., Bonsch, M., Humpenöder, F., Biewald, A., Stevanovic, M., 2014. Reactive nitrogen requirements to feed the world in 2050 and potential to mitigate nitrogen pollution. Nat. Commun. 5, 3858.

Cao, Z., Zhang, J., Deng, R., Wang, Z., Zhang, Z., Deng, B., Zhang, N., Zhang, Q., Wei, G., Liu, X., Xia, S., 2024. Enhanced ammonia recovery from wastewater by a transmembrane electro-chemisorption system directly connecting anode chamber and cathode chamber with gas permeable membrane. Chem. Eng. J. 485, 149554.

Chen, M., Zhao, X., Wang, C., Pan, S., Zhang, C., Wang, Y., 2021. Electrochemical oxidation of reverse osmosis concentrates using macroporous Ti-ENTA/SnO_2-Sb flow-through anode: degradation performance, energy efficiency and toxicity assessment. J. Hazard. Mater. 401, 123295.

Cruz, H., Law, Y.Y., Guest, J.S., Rabaey, K., Batstone, D., Laycock, B., Verstraete, W., Pikaar, I., 2019. Mainstream ammonium recovery to advance sustainable urban wastewater management. Environ. Sci. Technol. 53, 11066–11079.

Darestani, M., Haigh, V., Couperthwaite, S.J., Millar, G.J., Nghiem, L.D., 2017. Hollow fibre membrane contactors for ammonia recovery: current status and future developments. J. Environ. Chem. Eng. 5, 1349–1359.

Davey, C.J., Hermassi, M., Allard, E., Amine, M., Sweet, N., Gaite, T.S., McLeod, A., McAdam, E.J., 2020. Integrating crystallisation into transmembrane chemical absorption: process intensification for ammonia separation from anaerobic digestate. J. Membrane Sci. 611, 118236.

Deng, B., Zhang, Z., Zhang, J., Wang, Z., Wei, G., Jia, R., Xiang, P., Xia, S., 2023. Critical review in transmembrane electro-chemisorption technology for ammonia recovery from wastewater. Crit. Rev. Environ. Sci. Tec. 0, 1–22.

Deng, Z., van Linden, N., Guillen, E., Spanjers, H., van Lier, J.B., 2021. Recovery and applications of ammoniacal nitrogen from nitrogen-loaded residual streams: a review. J. Environ. Manage. 295, 113096.

Duan, H., Zhao, Y., Koch, K., Wells, G.F., Weißbach, M., Yuan, Z., Ye, L., 2021. Recovery of nitrous oxide from wastewater treatment: current status and perspectives. ACS EST Water 1, 240–250.

Erisman, J.W., Sutton, M.A., Galloway, J., Klimont, Z., Winiwarter, W., 2008. How a century of ammonia synthesis changed the world. Nat. Geosci. 1, 636–639.

Gonzalez-Salgado, I., Guigui, C., Sperandio, M., 2022. Transmembrane chemical absorption technology for ammonia recovery from wastewater: a critical review. Chem. Eng. J. 444, 136491.

Guida, S., Van Peteghem, L., Luqmani, B., Sakarika, M., McLeod, A., McAdam, E.J., Jefferson, B., Rabaey, K., Soares, A., 2022. Ammonia recovery from brines originating from a municipal wastewater ion exchange process and valorization of recovered nitrogen into microbial protein. Chem. Eng. J. 427, 130896.

Hou, D., Iddya, A., Chen, X., Wang, M., Zhang, W., Ding, Y., Jassby, D., Ren, Z.J., 2018. Nickel-based membrane electrodes enable high-rate electrochemical ammonia recovery. Environ. Sci. Technol. 52, 8930–8938.

Hou, D., Jassby, D., Nerenberg, R., Ren, Z.J., 2019. Hydrophobic gas transfer membranes for wastewater treatment and resource recovery. Environ. Sci. Technol. 53, 11618–11635.

Iddya, A., Hou, D., Khor, C.M., Ren, Z., Tester, J., Posmanik, R., Gross, A., Jassby, D., 2020. Efficient ammonia recovery from wastewater using electrically conducting gas stripping membranes. Environ. Sci.: Nano 7, 1759–1771.

Kim, K.-Y., Moreno-Jimenez, D.A., Efstathiadis, H., 2021. Electrochemical ammonia recovery from anaerobic centrate using a nickel-functionalized activated carbon membrane electrode. Environ. Sci. Technol. 55, 7674–7680.

Kim, K.-Y., Yang, W., Logan, B.E., 2018. Regenerable nickel-functionalized activated carbon cathodes enhanced by metal adsorption to improve hydrogen production in microbial electrolysis cells. Environ. Sci. Technol. 52, 7131–7137.

Kuchena, S.F., Wang, Y., 2020. Superior polyaniline cathode material with enhanced capacity for ammonium ion storage. ACS Appl. Energy Mater. 3, 11690–11698.

Kuntke, P., Rodríguez Arredondo, M., Widyakristi, L., ter Heijne, A., Sleutels, T.H.J.A., Hamelers, H.V.M., Buisman, C.J.N., 2017. Hydrogen gas recycling for energy efficient ammonia recovery in electrochemical systems. Environ. Sci. Technol. 51, 3110–3116. https://doi.org/10.1021/acs.est.6b06097.

Kuntke, P., Zamora, P., Saakes, M., Buisman, C.J.N., Hamelers, H.V.M., 2016. Gas-permeable hydrophobic tubular membranes for ammonia recovery in bio-electrochemical systems. Environ. Sci.: Water Res. Technol. 2, 261–265.

Kywe, P.P., Ratanatamskul, C., 2022. Influences of permeate solution and feed pH on enhancement of ammonia recovery from wastewater by negatively charged PTFE membranes in direct contact membrane distillation operation. ACS Omega 7, 27722–27733.

Li, J., Ma, J., Dai, R., Wang, X., Chen, M., Waite, T.D., Wang, Z., 2021a. Self-enhanced decomplexation of cu-organic complexes and Cu recovery from wastewaters using an electrochemical membrane filtration system. Environ. Sci. Technol. 55, 655–664.

Li, Y., Wang, R., Shi, S., Cao, H., Yip, N.Y., Lin, S., 2021b. Bipolar membrane electrodialysis for ammonia recovery from synthetic urine: experiments, modeling, and performance analysis. Environ. Sci. Technol. 55, 14886–14896.

Liu, B., Giannis, A., Zhang, J., Chang, V.W.-C., Wang, J.-Y., 2015. Air stripping process for ammonia recovery from source-separated urine: modeling and optimization. J. Chem. Technol. Biot. 90, 2208–2217.

Liu, X., Elgowainy, A., Wang, M., 2020. Life cycle energy use and greenhouse gas emissions of ammonia production from renewable resources and industrial by-products. Green Chem. 22, 5751–5761.

Mansourizadeh, A., Rezaei, I., Lau, W.J., Seah, M.Q., Ismail, A.F., 2022. A review on recent progress in environmental applications of membrane contactor technology. J. Environ. Chem. Eng. 10, 107631.

Massara, T.M., Malamis, S., Guisasola, A., Baeza, J.A., Noutsopoulos, C., Katsou, E., 2017. A review on nitrous oxide (N_2O) emissions during biological nutrient removal from municipal wastewater and sludge reject water. Sci. Total Environ. 596–597, 106–123.

Ren, G., Li, R., Zhao, M., Hou, Q., Rao, T., Zhou, M., Ma, X., 2023. Membrane electrodes for electrochemical advanced oxidation processes: preparation, self-cleaning mechanisms and prospects. Chem. Eng. J. 451, 138907.

Renard, J.J., Calidonna, S.E., Henley, M.V., 2004. Fate of ammonia in the atmosphere—A review for applicability to hazardous releases. J. Hazard. Mater. 108, 29–60.

Rodríguez Arredondo, M., Kuntke, P., ter Heijne, A., Hamelers, H.V.M., Buisman, C.J.N., 2017. Load ratio determines the ammonia recovery and energy input of an electrochemical system. Water Res. 111, 330–337.

Smith, C., K. Hill, A., Torrente-Murciano, L., 2020. Current and future role of Haber–Bosch ammonia in a carbon-free energy landscape. Energ. Environ. Sci. 13, 331–344.

Tarpeh, W.A., Barazesh, J.M., Cath, T.Y., Nelson, K.L., 2018. Electrochemical stripping to recover nitrogen from source-separated urine. Environ. Sci. Technol. 52, 1453–1460.

Wang, X., Daigger, G., de Vries, W., Kroeze, C., Yang, M., Ren, N.-Q., Liu, J., Butler, D., 2019a. Impact hotspots of reduced nutrient discharge shift across the globe with population and dietary changes. Nat. Commun. 10, 2627.

Wang, Z., Zhang, J., Guan, X., She, L., Xiang, P., Xia, S., Zhang, Z., 2019b. Bioelectrochemical acidolysis of magnesia to induce struvite crystallization for recovering phosphorus from aqueous solution. J. Environ. Sci. 85, 119–128.

Wang, Z., Zhang, J., Hu, X., Bian, R., Xv, Y., Deng, R., Zhang, Z., Xiang, P., Xia, S., 2020. Phosphorus recovery from aqueous solution via a microbial electrolysis phosphorus-recovery cell. Chemosphere 257, 127283.

Wang, Z., Zhang, Z., Zhang, J., She, L., Xiang, P., Xia, S., 2023. Concurrent recovery of ammonia and phosphate by an electrochemical nutrients recovery system with authigenic acid and base. Chem. Eng. J. 454, 140169.

Wu, H., Vaneeckhaute, C., 2022. Nutrient recovery from wastewater: a review on the integrated physicochemical technologies of ammonia stripping, adsorption and struvite precipitation. Chem. Eng. J. 433, 133664.

Yu, C., Huang, Xiao, Chen, H., Godfray, H.C.J., Wright, J.S., Hall, J.W., Gong, P., Ni, S., Qiao, S., Huang, G., Xiao, Y., Zhang, J., Feng, Z., Ju, X., Ciais, P., Stenseth, N.C., Hessen, D.O., Sun, Z., Yu, L., Cai, W., Fu, H., Huang, XiaoMeng, Zhang, C., Liu, H., Taylor, J., 2019. Managing nitrogen to restore water quality in china. Nature 567, 516–520.

Zhang, F., Ge, Z., Grimaud, J., Hurst, J., He, Z., 2013. Long-term performance of liter-scale microbial fuel cells treating primary effluent installed in a municipal wastewater treatment facility. Environ. Sci. Technol. 47, 4941–4948.

Zhang, J., Xie, M., Tong, X., Liu, S., Qu, D., Xiao, S., 2020. Recovery of ammonium nitrogen from human urine by an open-loop hollow fiber membrane contactor. Sep. Purif. Technol. 239, 116579.

Zhang, Z., Deng, R., Zhang, J., She, L., Wei, G., Jia, R., Xiang, P., Xia, S., 2024. Enhanced ammonia recovery from strong ammonia wastewater via a transmembrane electro-chemisorption system with authigenic acid and base. Desalination 571, 117099.

Zhang, Z., She, L., Zhang, J., Wang, Z., Xiang, P., Xia, S., 2019. Electrochemical acidolysis of magnesite to induce struvite crystallization for recovering phosphorus from aqueous solution. Chemosphere 226, 307–315.

Zhang, Z., Wang, Z., Zhang, J., Deng, R., Peng, H., Guo, Y., Xiang, P., Xia, S., 2021. Ammonia recovery from wastewater using a bioelectrochemical membrane-absorbed ammonia system with authigenic acid and base. J. Clean. Prod. 296, 126554.